https://dx.doi.org/10.1016/j.electacta.2018.09.128

Improved BDD Anode System in Electrochemical Degradation of *p*-nitrophenol by Corroding Electrode of Iron

Hongyu Li[a], Ke Wang[a], Xiuping Zhu[b], Yi Jiang[c], Xuan Xing[a*], Jianxin Xia[a*]

[a] Department of Environmental Science, College of Life and Environmental Science, Minzu University of China, Beijing 100081, China
[b] Department of Civil and Environmental Engineering, Louisiana State University, Baton Rouge, Louisiana 70803, United States
[c] Department of Civil and Environmental Engineering, The Hong Kong Polytechnic University, Hung Hom, Kowloon, Hong Kong

[*] Corresponding author. Tel.: +86 10 68933621.

E-mail: xingxuanpku@163.com. (X. Xing); *jxxia@vip.sina.com*

Abstract

A novel electrochemical system with corroding electrode of iron (Fe_c) inserted between boron-doped diamond (BDD) anode and carbon felt (CF) cathode, named BDD-Fe_c-CF system, was initially constructed and investigated in the present study. In this system, *p*-nitrophenol (*p*-NP) degradation was significantly enhanced in a wide pH range of 3~11 compared with BDD anode with CF cathode system (BDD-CF) and BDD anode with stainless steel (SS) cathode system (BDD-SS), respectively. Especially under acidic conditions, COD removal efficiency in BDD-Fe_c-CF system was achieved 89.1%, which was only 35.2% in BDD-SS system under the same conditions. The excellent performance under acidic conditions was mainly attributed to Electro-Fenton reaction. Hydroxyl radicals were formed by reaction between Fe^{2+} released from Fe_c electrode and H_2O_2 generated by dissolved oxygen reduction at CF cathode. Under alkaline conditions, flocs were formed to remove *p*-NP by coagulation besides anode oxidation, electro-generated oxidants and Fe(VI) oxidation. The fate of Fe ions was examined whose releasing rate was influenced by strength of electronic field and pH of solution. Under acidic conditions, Fe^{2+} released from Fe_c was oxidized into Fe^{3+} and then was adsorbed and reduced at CF cathode. Under alkaline conditions, flocs were formed by reaction between Fe^{2+} and hydroxyl which came from oxygen reduction.

Keywords: Boron-doped Diamond; Corroding Electrode of Iron; *p*-nitrophenol; Electrochemical Oxidation; Electro-Fenton.

1. Introduction

Electrochemical oxidation has become the most promising technology for treating wastewater containing bio-refractory organic pollutants because it is environmentally friendly, oxidation efficient, easy to control, and universally applied [1-5]. The anode material is a key factor to improve the effectiveness and efficiency of an electrochemical oxidation system. Many materials have been investigated including Pt [6], IrO_2 [7], RuO_2 [3], PbO_2 [8], SnO_2 [9] and boron-doped diamond (BDD) anodes [2]. Because of several unique technological properties, such as an extremely wide potential window, corrosion stability in aggressive media, inert surface with low adsorption properties, and strong oxidation capability, the BDD anode system has been widely used to treat wastewater containing surfactants, herbicides, dyes, and endocrine disrupting chemicals [10-12].

In order to improve the oxidation ability, Electro-Fenton systems have been constructed for effective pollutants degradation. The basic principle of a Electro-Fenton system is shown below (Eqs. 1 and 2).

$$O_2 + 2\,H^+ + 2\,e^- \rightarrow H_2O_2 \qquad (1)$$

$$Fe^{2+} + H_2O_2 + H^+ \rightarrow Fe^{3+} + \cdot OH + H_2O \qquad (2)$$

H_2O_2 is generated in situ by reducing dissolved oxygen on carbonaceous cathode materials, such as graphite felt [13], ordered mesoporous carbon [14], carbon nanotubes [15], active carbon fiber [16], and carbon felt (CF) [17]. More ·OH is expected to be produced in the presence of Fe^{2+} according to Eq. (2), which significantly improves the oxidation ability of the system. Avoiding some limitations

of the classical Fenton reaction, such as the risk related to transport and storage of H_2O_2, the Electro-Fenton system with a BDD anode and a CF cathode has been successfully applied in organic pollutants degradation. For instance, Isarain-Chavez et al. [18] utilized an Electro-Fenton system to degrade the β-blocker metoprolol tartrate by adding 0.5 mmol Fe^{2+} and 80% of total organic carbon was removed in 360 min. Another study [19] showed that the concentration of sulfachloropyridazine (SCP) was reduced from 0.21 mmol to 0 mmol after 40 min during Electro-Fenton degradation of SCP after adding 0.2 mmol Fe^{2+}.

Although the Electro-Fenton systems with a BDD anode and a CF cathode had superior performance for bio-refractory organic pollutants degradation, some drawbacks have hampered its large-scale application: (*i*) the pH value of the solution for this method is very narrow, usually should be controlled at 3. (*ii*) Fe^{2+} need to be added into Electro-Fenton systems to catalyze H_2O_2 into ·OH and the high cost of ferrous salts ran up the cost of this method. (*iii*) A large amount of iron mud is inevitably produced. Pignatello et al. [20] reported that Fe(III) oxyhydroxides was formed during the Electro-Fenton reaction. Therefore, it is imperative to develop a novel way to introduce Fe^{2+} into the BDD anode system to perform at its best without external investment.

In this study, a novel electrochemical system with BDD anode, CF cathode, and a sheet of iron was constructed (BDD-Fe_c-CF). The iron was defined as corroding electrode (Fe_c), which was inserted between the anode and cathode without electronic charge connection. Fe^{2+} can be released into the system under the affection of

electronic field and solvent environment. The performance and mechanisms of the BDD-Fe_c-CF system for *p*-nitrophenol (*p*-NP) degradation was explored under different pH conditions [21]. The oxidation ability of each part in the system such as anode, electro-generated oxidants, Electro-Fenton and Fe(VI) was quantified. The fate of Fe in the system was also analyzed by evolution of the amount of Fe^{2+}, Fe^{3+} and total Fe under different current densities and pH conditions. Phenolic compounds are widely used in metallurgy, petroleum, chemicals, textiles, dye printing, paper making, and pharmaceuticals [22-24] and are persistent, highly toxic, non-biodegradable, and discharged into the environment without being handled properly [25-27]. Therefore, *p*-NP was selected as the model organic compound to be removed by the BDD-Fe_c-CF system in this study.

2. Experimental

2.1 Chemicals

All chemicals were analytical grade and purchased from Sigma-Aldrich. Sodium sulfate was used as supporting electrolyte. Sulfuric acid and sodium hydroxide were used for pH adjustment. Solutions were prepared by ultrapure water obtained from Milli-Q Integral system (resistivity > 18 MΩ cm^{-1}) (Millipore Corp. Bedford, MA, USA) at room temperature. BDD anode was bought from CONDIAS GmbH (Itzehoe, Germany) with a size of 20 mm × 20 mm × 1 mm. Stainless steel (SS) sheet (Liduboyi Technologies, Beijing, China) and CF (Sigma-Aldrich) with the same size were used as cathode, respectively. Iron sheet (Liduboyi Technologies, China) with the same size was used as Fe_s. Before electrolysis, CF electrode was soaked in NaOH

(4.5 M) and HCl (5 M) for 10 min respectively and then washed by ultrapure water for three times.

2.2 Bulk Electrolysis

Bulk electrolysis of all *p*-NP was performed in a reactor under galvanostatic conditions with the current density of 20 mA cm^{-2}. The bulk electrolysis was processed under room temperature (25℃). BDD electrode was used as anode with SS and CF used as cathode, respectively. Fe_c with the same size was inserted between the anode and the cathode without electronic charge. The gap between two electrodes was set to be 10 mm. The concentration of *p*-NP was 1 mM, with 0.2 M Na_2SO_4 used as supporting electrolyte. 250 mL solution was stirred with a magnetic stirring bar during electrolysis. Samples were collected at each interval time and prepared for analysis.

2.3 Analytical methods

p-NP was quantified by high performance liquid chromatography (HPLC) (Shimadzu Scientific Instruments, Tokyo, Japan) with a ZORBAX SB-C18 analytical column (4.6 mm × 250 mm × 5 μm) and a diode array detector. The mobile phase was the mixture of methanol and ultrapure water with ratio of 60%:40% and flow rate was controlled at 1 mL min^{-1}. Column temperature was controlled at 25℃. The wavelength for the UV detector was set to 314 nm for *p*-NP detection. Chemical oxygen demand (COD) was measured by the potassium dichromate titrimetric method with a COD digestion instrument (INESA, Shanghai, China) at 150℃ for 2 h.

Flocs were analyzed by Fourier transform-infrared (FT-IR) spectroscopy (VERTEX 70; Bruker, Billerica, MA, USA) and embedded in KBr pellets at a

scanning wave range of 4,000~400 cm^{-1}. The X-ray photoelectron spectroscopy (XPS) analyses (ESCALAB 250) were performed with an Mg K_α source (Thermo Scientific, Waltham, MA, USA) and recorded in the range of 0~1,300 eV.

Intermediates of *p*-NP degradation were identified by gas chromatography (GC) (Agilent 6890; Agilent Technologies, Palo Alto, CA, USA) and mass spectrometry (MS) (Agilent 5973). Separation was achieved by an HP-5MS column (0.25 mm × 30 m × 0.25 μm). The GC conditions were as followings: helium was used as carrier gas with flow rate of 1 mL min^{-1}; injector temperature was set 280℃; oven temperature was initially 40℃ and kept for 10 min, then increased to 300℃ by the rate of 5℃ min^{-1} and held for 5 min. The effluent from the GC column was connected to the MS. The spectra were obtained by EI mode with 2,000 eV ionization energy and 35~500 amu scan for 2 s. The degradation products were identified by comparation with the mass spectra library stored in the MS system.

N,N-Dimethyl-p-nitrosoaniline (RNO) was used as a spin trap for hydroxyl radicals [18] and it was measured by a UV-vis spectrophotometer (V-750, JASCO, Tokyo, Japan) at 440 nm. The volume of electrolyte was 250 mL, which contained 0.2 M Na_2SO_4 and 3×10^{-5} M RNO. Electrolysis was performed under room temperature (25℃) with constant current density of 20 mA cm^{-2} for 20 min. The pH value of electrolyte solution was adjusted by 5 M H_2SO_4 and 5 M NaOH, respectively. The solution was stirred with a magnetic stir bar.

I^-/I_2 assays were performed to measure electrogenerated oxidants. The volume of electrolyte was 250 mL, which contained 0.2 M Na_2SO_4. Electrolysis was performed

with constant current density of 20 mA cm^{-2} under room temperature (25 °C) for 20 min. BDD electrode was used as anode and SS was used as cathode. The gap between electrodes was set to be 10 mm. Sample with the volume of 10 mL was collected from the electrolysis cell every 5 min. 5 mL of HCl and 10 mL of 0.01 M KI (1:1) were added into the sample immediately. After that, the sample was stored in the dark for 15 min. Finally, 0.005M $Na_2S_2O_3$ was used to titrate the amount of I_2 with the indictor of starch. The concentration of electrogenerated oxidants (C_{EO}) was calculated using the following equation:

$$C_{EO}(mM) = \frac{V_{S_2O_3^{2-}} - C_{S_2O_3^{2-}}}{4V_{sample}} \quad (3)$$

where V_{S2O3}^{2-} is the volume of $Na_2S_2O_3$ solution used for titration (in mL), C_{S2O3}^{2-} is the concentration of $Na_2S_2O_3$ solution (in mM), V sample is the volume of collected sample (in mL), and 4 is a factor for charge conservation (1 mol O_2 mol^{-1} e^{-1} /4 mol $S_2O_3^{2-}$ e^{-1})

Fe ions were determined by the ferrozine method. A fuchsia complex was formed by Fe^{2+} and ferrozine (1 mmol), which was detected at 562 nm with a UV-vis spectrophotometer. The amount of Fe^{2+} was determined by the concentration of the fuchsia complex. Fe^{3+} was first reduced to Fe^{2+} with ascorbic acid and then measured by the ferrozine method to calculate the amount of total Fe. Furthermore, the amount of Fe^{3+} can be estimated by the difference between total Fe and Fe^{2+}.

3. Results and discussion

3.1 *p*-NP and COD degradation performance

Three systems of BDD anode with SS cathode (BDD-SS), BDD anode with CF cathode (BDD-CF) and BDD-Fe_c-CF were constructed and compared in a wide pH range. The pH value was set to be 5.6 (original pH value of *p*-NP solution), 3 and 11 with 1 mM *p*-NP, 0.2 M Na_2SO_4, and a current density of 20 mA cm^{-2} for bulk electrolysis (Figure 1).

p-NP removal efficiency was also monitored for 5 h at 0 $mA \cdot cm^{-2}$ to distinguish the effect of CF cathode adsorption (Supporting Information Figure S1), which demonstrated that adsorption of *p*-NP on CF cathode was negligible.

[Figure 1]

Figure 1 (a) showed degradation of *p*-NP under original conditions as a function of electrolysis time. *p*-NP was rapidly removed in BDD-CF and BDD-Fe_c-CF systems in 2 h. However, in BDD-SS system, after 5 h of electrolysis still 8% *p*-NP was left.

The comparation of COD decrease was shown in Figure 1 (b). Results showed that after 5 h of electrolysis, COD removal efficiency in BDD-SS system was 53.7%. However, the removal efficiency was achieved 64.5% in BDD-CF system. The promotion was mainly due to generation of H_2O_2 at CF cathode (Eq. 1) [28]. Furthermore, COD removal efficiency in BDD-Fe_c-CF system was also improved, which reached 68.8% after 5 h electrolysis. The enhancement was mainly due to a Fenton-like reaction between Fe^{2+}, which was released from Fe_c electrode, and H_2O_2 generated at CF cathode. The Fenton-like reaction occurred under original conditions

was not as strong as that under acidic conditions, but still had contribution for COD decrease [29].

Under acidic conditions of pH 3, *p*-NP was completely removed in only 1 h in BDD-CF and BDD-Fe_c-CF systems as shown in Figure 1 (c), which was mainly due to Fenton reaction on organic pollutants' degradation (Eq. 1 and Eq. 2) [30]. Still 10% *p*-NP was left after 5 h electrolysis in BDD-SS system.

89.1% of COD was removed after 5 h electrolysis in BDD-Fe_c-CF system (Figure 1 (d)), which improved 20.3% compared with original conditions. In BDD-CF system, COD mineralization rate was 68.2% after 5 h electrolysis. Which was similar with original conditions. However, in BDD-SS system, only 35.2% of COD was removed, which was much lower than that of 53.6% under original conditions. This phenomenon demonstrated that under acidic conditions BDD anode oxidation of *p*-NP was reduced while Fenton reaction significantly enhanced the oxidation ability of the system. Current efficiency (CE) of the three systems was also analyzed (Supporting information Figure S2). Affected by *p*-NP concentration, CE decreased along with electrolysis time and the highest value was achieved at the first electrolysis hour [31]. In BDD-Fe_c-CF system, the highest value of CE was 79.1%, which was much higher than that of 49.8% in BDD-CF system and 32.2% in BDD-SS system.

The behavior of the BDD-Fe_c-CF system under alkaline conditions (pH=11) was investigated with many flocs generated. The removal percentages of *p*-NP and COD were analyzed with flocs dissolved in H_2SO_4 (5 M) or removed by centrifugation, respectively. After 5 h of electrolysis, 99.9% *p*-NP and 88.5% COD were eliminated

with flocs removed by centrifugation (Figure 1 (e) and Figure 1 (f)). When flocs were dissolved by H_2SO_4, COD mineralization decreased to 81.4%, which meant the flocs coagulation played an important role on COD removing. However, the mineralization rate of COD in the BDD-Fe_c-CF system with flocs dissolved was still 8.8% higher compared with BDD-CF system, in which COD removal percentage achieved 72.6% after 5 h electrolysis. The higher mineralization rate of BDD-Fe_c-CF system was mainly due to oxidation by Ferrate (Fe(VI)) formed under alkaline condition. Ferrous released from the iron anode can be further oxidized into Fe(VI) under alkaline conditions in electrolysis systems, which has strong oxidation ability for organic compounds [32]. In BDD-SS system, electrochemical oxidation was only due to BDD anode oxidation with the degradation efficiency of *p*-NP 89.2% and COD 37.4% after 5 h of electrolysis.

3.2 Degradation contribution identification

Based on the present study, the BDD-Fe_c-CF system removed organic compounds efficiently in a wide pH range with varied degradation mechanisms. The anodic oxidation (AO), electro-generated oxidants (EO), Electro-Fenton (EF), coagulation, and Fe(VI)-oxidation were observed in the BDD-Fe_c-CF system under original, acidic, and alkaline conditions. In order to identify the contributions of each oxidation component, COD removal percentage in different systems was compared and used as the index. All the results were shown in Figure 2.

[Figure 2]

First, the contribution of anodic oxidation was identified. In BDD-SS system,

COD removal was only due to anode oxidation. At cathode, hydrogen was formed by hydrogen ions reduction. Therefore, the COD removal percentages by anodic oxidation ($COD_{AO} = COD_{BDD\text{-}SS}$) were 53.7% (original conditions), 35.2% (acidic conditions), and 37.4% (alkaline conditions), respectively (Figure 2). These results suggested that the contribution of anodic oxidation for *p*-NP under the original conditions was stronger than that under acidic or alkaline conditions, which was consistent with previous study [33].

Second, the oxidation ability of EO was identified by the difference of COD removal percentages between BDD-SS and BDD-CF systems. Many kinds of oxidants, such as H_2O_2, were produced at CF cathode. Therefore, both anodic oxidation and EO existed in BDD-CF system. The contributions of EO ($COD_{EO} = COD_{BDD\text{-}CF} - COD_{BDD\text{-}SS}$) were 10.8% (original conditions), 33% (acidic conditions), and 35.2% (alkaline conditions), respectively.

Third, Electro-Fenton oxidation enhanced the oxidation ability in BDD-Fe_c-CF system under original and acidic conditions. However, it was difficult to identify the exact quantity of H_2O_2 attended the Electro-Fenton reaction, especially under original conditions [34]. Thus, the difference of COD removal efficiency between BDD-Fe_c-CF system and BDD-CF system didn't represent the Electro-Fenton affection, but the improvement for oxidation ability by Electro-Fenton reaction ($COD_{EF} = COD_{BDD\text{-}Fes\text{-}CF} - COD_{BDD\text{-}CF}$). The improvement calculated by COD decrease were 4.3% (original conditions) and 20.9% (acidic conditions).

Fourth, the contribution of coagulation for COD decrease was identified by

comparing the COD removal percentages after flocs centrifugation and dissolution ($COD_{Flocs} = COD_{flocs\ centrifuged} - COD_{flocs\ dissolved}$). The results showed that COD removal percentages were 88.5% with flocs centrifugated and 81.4% with flocs dissolved, which indicated contribution of coagulation for COD removal was 7.1% in BDD-Fe_c-CF system under alkaline conditions.

Finally, based the difference of COD removal percentages between BDD-Fe_c-CF system with flocs dissolved (81.4%) and BDD-CF system (72.6%) under alkaline conditions, Fe(VI)-oxidation was proposed to be existed in the system. The formation and detection for Fe(VI) in electrochemical systems under alkaline conditions have been extensively reported before (Eq. (4)), which has been identified as a "green" oxidant for drinking water and wastewater treatment [35, 36].

$$Fe + 8\ OH^- \rightarrow FeO_4^{2-} + 4\ H_2O + 6\ e^- \qquad (4)$$

The contribution of Fe(VI)-oxidation was calculated ($COD_{Fe(VI)} = COD_{flocs\ dissolved} - COD_{BDD\text{-}CF}$) to be 8.8% in BDD-$Fe_s$-CF system under alkaline conditions.

In summary, the aforementioned mechanisms of anodic oxidation, electro-generated oxidants, Electro-Fenton, coagulation, and Fe(VI)-oxidation in the BDD-Fe_c-CF system were identified and quantified in terms of contributions to COD removal percentages in a wide pH range of 3~11(Figure 2). Anodic oxidation was the main action under the original conditions due to the strong oxidation ability of the BDD anode. The joint actions of Electro-Fenton and electro-generated oxidants also had great contribution especially under acidic conditions. The synergies of flocs coagulation and Fe(VI)-oxidation enhanced COD removal under alkaline conditions.

3.3 Electro-generated oxidants and intermediates

The production of ·OH and electro-generated oxidants in the BDD-Fe_c-CF system were quantified under different pH conditions (Figure 3). Concentration of ·OH was analyzed by the RNO method and electro-generated oxidants was measured by I^-/I_2 assays. As shown in Figure 3(a), ·OH increased gradually with electrolysis time under all pH conditions. Especially under acidic conditions, ·OH achieved the highest concentration because of the Electro-Fenton reaction. However, under original and alkaline conditions, Fenton reaction was hampered and the concentration of ·OH was lower [37].

.[Figure 3]

Electro-generated oxidants including H_2O_2 and peroxodisulfates ($S_2O_8^{2-}$) were also analyzed in BDD-Fe_c-CF system. $S_2O_8^{2-}$ was formed by oxidation of sulfates (SO_4^{2-}) at BDD anode, which could be further decomposed into sulfate radicals ($SO_4^{\cdot-}$) (Eq. (5)) [38]. As shown in Fig 3(b), the concentration of electro-generated oxidants increased with reaction time under all pH conditions. What's more, the highest concentration was still achieved under acidic conditions, which was mainly due to the high concentration of H_2O_2 formed at the CF cathode (Eq. (1)) [39, 40]. A lot of oxidants formed under acidic conditions was consistent with the rapid mineralization of *p*-NP in the BDD-Fe_c-CF system.

$$Fe^{2+} + S_2O_8^{2-} \rightarrow Fe^{3+} + SO_4^{2-} + SO_4^{\cdot-} \qquad (5)$$

Intermediates of *p*-NP degradation were analyzed by GC-MS (Supporting Information Table S1) and the primary degradation pathway was proposed

(Supporting Information Figure S3). Hydroquinone and *p*-benzoquinone were formed and their formation indicated that carbon atom connected with -NO_2 was attacked by oxidants first. This result was consistent with previous research which pointed out that carbon atom connected with -NO_2 had the highest electron density among the benzene ring [41]. The concentrations of hydroquinone and *p*-benzoquinone were analyzed during electrolysis by HPLC (Supporting Information Figure S4). As results, their concentrations increased first along with the disappearance of *p*-NP and then they were decomposed for further mineralization.

3.4 Fate of Fe ions in the BDD-Fe_s-CF system

In BDD-Fe_c-CF system, the behavior of Fe ions can be divided into three steps under acidic conditions (Figure 4). First, Fe^{2+} was generated from Fe_c electrode and the releasing rate was influenced by strength of the electric field and pH value of solution. Under the effect of electric field, electrons were redistributed in Fe_c electrode, which were concentrated towards BDD anode side. At the same time, a large amount of H^+ was reduced to H_2 at the Fe_c electrode surface when pH of the solution was adjusted to 3 (shown in Eq. (6)). Second, Fe^{2+} was oxidized into Fe^{3+} by dissolved oxygen as reported by Divager (Eq. (7)) [42]. Therefore, both Fe^{2+} and Fe^{3+} existed in the solution. Finally, Fe^{2+} and Fe^{3+} were absorbed on the CF cathode and Fe^{3+} was reduced to Fe^{2+} due to its negative charge and large porous surface according to Long (Eq. (8)) [43].

[Figure 4]

The concentrations of Fe^{2+} and Fe^{3+} at different current densities as a function of

electrolysis time were analyzed under acidic conditions (Figure 5 (a) and (b)). Fe^{2+} and Fe^{3+} were generated and their concentrations increased with time even without current supply because of the reaction of Eq. (6). Concentration of dissolved oxygen was saturated during the reaction by stirring with a magnetic stir bar (Supporting Information Figure S5), which would oxidize Fe^{2+} to Fe^{3+} immediately (Eq. (7)). After 5 h reaction, the concentration of Fe^{2+} reached 1.62 mM, whereas that of Fe^{3+} reached 3.32 mM. The amount of Fe^{2+} to Fe^{3+} both increased with the electric field strengthened by increasing current density. When current density increased from 0 to 20 mA cm^{-2}, concentration of Fe^{2+} was promoted from 1.62 to 2.19 mM after 5 h reaction. In the meantime, Fe^{3+} accumulated from 3.32 to 4.2 mM in the solution.

$$Fe + 2\,H^{+} \rightarrow Fe^{2+} + H_2\uparrow \qquad (6)$$

$$4\,Fe^{2+} + O_2 + 4\,H^{+} \rightarrow 4\,Fe^{3+} + 2\,H_2O \qquad (7)$$

After releasing from Fe_c electrode, Fe^{2+} and Fe^{3+} were not stable in the solution and will further reacted with CF cathode. In order to analyze the amount of Fe^{2+} and Fe^{3+} attached to CF cathode, the cathode was washed with H_2SO_4 (5 M) and the amounts of Fe^{2+} and Fe^{3+} were shown in Figure 5(c). Most of the iron ions attached on CF cathode were Fe^{2+} with only a few Fe^{3+} ions existed, which consisted of the reaction shown in Eq. (8). Meanwhile, the amount of iron ions accumulated on CF cathode was also related with the current density and their quantity increased with increasing current density. After 5 h reaction, the quantity of Fe^{2+} and Fe^{3+} were 4.02 mM and 0.29 mM at the cathode with a current density of 20 mA·cm^{-2}, respectively.

$$Fe^{3+} + e^{-} \rightarrow Fe^{2+} \qquad (8)$$

The pH of the BDD-Fe_s-CF system increased along with reaction time, which was supported by the consumption of H^+ (Eq. (6)). The pH value was also affected by the strength of electronic field, which increased with increasing current density at the same electrolysis time (Figure 5(d)). This phenomenon agreed with the effect of electronic field on Fe^{2+} releasing. Both Fe^{2+} and Fe^{3+} were generated in the BDD-Fe_c-CF system which catalyzed H_2O_2 into ·OH (Fenton Reaction). Consequently, the oxidation capacity of the BDD-Fe_c-CF system under acidic conditions was greatly enhanced.

[Figure 5]

Unexpected, *p*-NP removal efficiency in BDD-Fe_c-CF system under alkaline conditions was comparable with that under acidic conditions. The efficient degradation was mainly due to the generation of flocs. Influenced by electronic field, electrons were redistributed and concentrated towards the anode side in Fe_c (Figure 4). Then, O_2 was reduced into OH^- at the same site (Eq. (9)). $Fe(OH)_2$ was formed by the reaction between Fe^{2+} and OH^- as shown in Eq. (10). Furthermore, $Fe(OH)_3$ was produced by the reaction of $Fe(OH)_2$ and O_2 (Eq. (11)). During the experiment, a thick reddish layer of flocs was attached on the side of Fe_c electrode towards CF cathode. These flocs are speculated to be a mixture of $Fe(OH)_2$ and $Fe(OH)_3$.

$$O_2 + 2\ H_2O + 4\ e^- \rightarrow 4\ OH^- \qquad (9)$$

$$Fe^{2+} + 2\ OH^- \rightarrow Fe(OH)_2 \qquad (10)$$

$$4\ Fe(OH)_2 + O_2 + 2\ H_2O \rightarrow 4\ Fe(OH)_3 \qquad (11)$$

Besides flocs, Fe(VI), which has been demonstrated to be efficient for

mineralizing organic compounds, was also formed in the BDD-Fe_c-CF system under alkaline conditions. Sun et al. [44] used sponge iron as an anode, and the electrochemically generated Fe(VI) was capable of degrading more than 70% phenol within 45 min at pH 9. However, because of the large surface area of the flocs, most of Fe(VI) was adsorbed on the flocs and could not be separated in the BDD-Fe_c-CF system. For this reason, the mineralization of Fe(VI) was verified according to the difference on COD removal between BDD-Fe_c-CF system with flocs removed and BDD-CF system, which has been discussed in above degradation mechanism section (Figure 2).

In order to determine the quantity of iron ions released into the system under alkaline conditions, the entire system was soaked in H_2SO_4 (5 M) solution for 3 h after 1 h electrolysis. All of the flocs were dissolved and quantified by the ferrozine method. The results showed that almost 12.9 mM iron ions were released after 1 h electrolysis without current supply and their concentration grew with current density increasing (Figure 6).

[Figure 6]

The flocs that formed during electrolysis process were analyzed by XPS (Supporting Information Figure S6) and FT-IR (Supporting Information Figure S7) to further confirm their compositions. The two XPS peaks at 725 and 711 eV with a peak area ratio of 2:1 were assignable to Fe 2p1/2 and Fe 2p3/2, which was consistent with a previous report [45]. It is confirmed that the flocs were mainly composed of iron oxides. Other atoms in the flocs, such as C, N, and O, indicated that the flocs also

contained aggregations of organic compounds.

The peak of FT-IR spectra at 3,450 cm^{-1} corresponding to -OH was due to the substituent group of -OH on *p*-NP. The peak at 1,639 cm^{-1} was a double bond (C=C) in benzene ring, and the peak at 1,118 cm^{-1} belonged to C-O in *p*-NP molecular structure. The characteristic peak corresponding to the stretching vibration of the Fe–O bond was the peak at 618 cm^{-1}. These results confirmed that the flocs were a mixture of iron oxides and organic compounds, demonstrating that the flocs contributed to organic pollutant removal.

4. Conclusions

The performance of *p*-NP degradation was significantly improved in BDD-Fe_c-CF system in a wide pH range of 3~11. Under acidic conditions, Electro-Fenton reaction between Fe^{2+} was released from Fe_c electrode and H_2O_2 generated at CF cathode enhanced the oxidation ability. Under alkaline conditions, flocs composed by $Fe(OH)_2$ and $Fe(OH)_3$ were formed to remove organic compounds by coagulation. The releasing rate of Fe^{2+} from Fe_c was influenced by both of strength of electronic field and pH of the electrolyte. Joint action of anodic oxidation, electro-generated oxidants oxidation, Electro-Fenton reaction under acidic conditions, as well as coagulation and Fe(VI)-oxidation under alkaline conditions has improved *p*-NP degradation in the BDD-Fe_c-CF system, which made it more efficient for wastewater treatment compared with traditional electrochemical oxidation system.

Acknowledgements

This research was supported by National Natural Science Foundation of China (No.51409285) and Collaborative Innovation Center for Ethnic Minority Development of China.

References

[1] M. Michele, A. Vacca, S. Palmas, Electrochemical treatment as a pre-oxidative step for algae removal using Chlorella vulgaris, as a model organism and BDD anodes, Chem. Eng. J. 219 (2013) 512.

[2] X. P. Zhu, J. R. Ni, The improvement of boron-doped diamond anode system in electrochemical degradation of p-nitrophenol by zero-valent iron, Electrochim. Acta. 56 (2011) 10371.

[3] D. P. Dubal, G. S. Gund, R. Holze, H. S. Jadhav, C. D. Lokhande, C-Jin. Park, Solution-based binder-free synthetic approach of RuO_2, thin films for all solid state supercapacitors, Electrochim. Acta. 103 (2013) 103.

[4] C.A. Martinez-Huitle, M.A. Rodrigo, I. Sires, O. Scialdone, Single and Coupled Electrochemical Processes and Reactors for the Abatement of Organic Water Pollutants: A Critical Review, Chem. Rev. 115 (2015) 13362.

[5] P.V. Nidheesh, R. Gandhimathi, Trends in Electro-Fenton process for water and wastewater treatment: An overview, Desalination. 299 (2012) 1.

[6] M. Panizza, G. Cerisola, Application of diamond electrodes to electrochemical processes, Electrochim. Acta. 51 (2005) 191.

[7] Y. J. Feng, X. Y. Li, Electro-catalytic oxidation of phenol on several metal-oxide electrodes in aqueous solution, Water Res. 37 (2003) 2399.

[8] M. Panizza, G. Cerisola, Electrochemical degradation of methyl red using BDD and PbO_2 anodes, Ind. Eng. Chem. Res. 47 (2008) 6816.

[9] Y. H. Sun, P. P. Dong, X. Lang, J. M. Nan, Comparative study of electrochemical

performance of SnO_2 anodes with different nanostructures for lithium-Ion batteries, J. Nanosci. Nanotechnol. 15 (2015) 5880.

[10] M. E. Henry. Bergmann, J. Rollin, T. Iourtchouk, The occurrence of perchlorate during drinking water electrolysis using BDD anodes， Electrochim. Acta. 54 (2009) 2102.

[11] D. Gandini, E. Mahe, P. A. Michaud, W. Haenni, A. Perret, C. Comninellis, Oxidation of carboxylic acids at boron-doped diamond electrodes for wastewater treatment, J. Appl. Electrochem. 30 (2000) 1345.

[12] B. Marselli, J. Garcia-Gomez, P. A. Michaud, M. A. Rodrigo, C. Comninellis, Electrogeneration of Hydroxyl Radicals on Boron-Doped Diamond Electrodes, J. Electrochem. Soc. 150 (2003) D79.

[13] S. Yuan, Z. Li, Y. Wang, Effective degradation of methylene blue by a novel electrochemically driven process, Electrochem. Commun. 29 (2013) 48.

[14] L. Zhou, Z. X. Hu, C. Zhang, Z. H. Bi, T. Jin, M. H. Zhou, Electrogeneration of hydrogen peroxide for Electro-Fenton system by oxygen reduction using chemically modified graphite felt cathode, Sep. Purif. Technol. 111 (2013) 131.

[15] Y. P. Sheng, S. Song, X. L. Wang, H. H. Sun, X. Q. Niu, Electrogeneration of hydrogen peroxide on a novel highly effective acetylene black-PTFE cathode with PTFE film, Electrochim. Acta. 56 (2011) 8651.

[16] L. Wang, M. Cao, Z. Ai, L. Zhang, Design of a highly efficient and wide pH Electro-Fenton oxidation system with molecular oxygen activated by ferrous-tetrapolyphosphate complex, Environ. Sci. Technol. 49 (2015) 3032.

[17] A. Özcan, Y. Sahin, A. Savas. Koparal, M. A. Oturan. Carbon sponge as a new cathode material for the Electro-Fenton process: Comparation with carbon felt cathode and application to degradation of synthetic dye basic blue 3 in aqueous medium, J. Electroanal. Chem. 616 (2008) 71.

[18] E. Isarain-Chávez, C. Arias, P. Lluis. Cabot, F. Centellas, R. Maria. Rodriguez, J. Antonio. Garrido, E. Brillas, Mineralization of the drug β-blocker atenolol by Electro-Fenton and photoelectro-Fenton using an air-diffusion cathode for H_2O_2 electrogeneration combined with a carbon-felt cathode for Fe^{2+} regeneration, Appl. Catal. B-Environ. 96 (2010) 361.

[19] M Haidar, A. Dirany, I. Sires, N. Oturan, M. A. Oturan, Electrochemical degradation of the antibiotic sulfachloropyridazine by hydroxyl radicals generated at a BDD anode, Chemosphere. 91 (2013) 1304.

[20] J. Joseph. Pignatello, E. Oliveros, A. MacKay. Advanced Oxidation Processes for Organic Contaminant Destruction Based on the Fenton Reaction and Related Chemistry, Crit. Rev. Env. Sci. Technol. 36 (2006) 1.

[21] M.A. Quiroz, S. Reyna, C.A. Martinez-Huitle, S. Ferro, A. De Battisti, Electrocatalytic oxidation of p-nitrophenol from aqueous solutions at Pb/PbO_2 anodes, Appl. Catal. B-Environ. 59 (2005) 259.

[22] W. A. Hashemi, M. A. Maraqa, M. V. Rao, M. M. Hossain, Characterization and removal of phenolic compounds from condensate-oil refinery wastewater, Desalin. Water. Treat. 54 (2015) 660.

[23] B. K. Korbahti, A. Tanyolac, Kinetic Modeling of Conversion Products in the

Electrochemical Treatment of Phenolic Wastewater with a NaCl Electrolyte, Ind. Eng. Chem. Res. 42 (2009) 5060.

[24] K. Farhod. Chasib, Extraction of Phenolic Pollutants (Phenol and p-Chlorophenol) from Industrial Wastewater, J. Chem. Eng. Data. 58 (2013) 1549.

[25] M. Achak, A. Hafidi, L. Mandi, N. Ouazzani, Removal of phenolic compounds from olive mill wastewater by adsorption onto wheat bran, Desalin. Water. Treat. 52 (2014) 2875.

[26] J. Araña, R. E. Tello, J. M. Dona. Rodriguez, J. A. Herrera. Melian, D. O. Gonzalez, P. J. Perez, Highly concentrated phenolic wastewater treatment by the photo-Fenton reaction, mechanism study by FTIR-ATR, Chemosphere. 44 (2001) 1017.

[27] A. El-Ghenymy, F. Centellas, R. Maria. Rodriguez, P. Lluis. Cabot, J. Antonio. Garrido, L. Sires, E. Brillas, Comparative use of anodic oxidation, Electro-Fenton and photoelectro-Fenton with Pt or boron-doped diamond anode to decolorize and mineralize Malachite Green oxalate dye, Electrochim. Acta. 182 (2015) 247.

[28] F. Yu, M. Zhou, L. Zhou, R. Peng, A Novel Electro-Fenton Process with H_2O_2 Generation in a Rotating Disk Reactor for Organic Pollutant Degradation, Environ. Sci. Technol. Lett. 1 (2014) 320.

[29] A. Fischbacher, S. C. Von, T. C. Schmidt. Hydroxyl radical yields in the Fenton process under various pH, ligand concentrations and hydrogen peroxide/Fe(II) ratios, Chemosphere. 182 (2017) 738.

[30] L. Xu, J. Wang. Fenton-like degradation of 2,4-dichlorophenol using Fe_3O_4,

magnetic nanoparticles, Appl. Catal. B-Environ. 123–124 (2012) 117.

[31] X. Xing, J. Ni, X. Zhu, Y. Jiang, J. Xia. Maximization of current efficiency for organic pollutants oxidation at BDD, Ti/SnO_2-Sb/PbO_2, and Ti/SnO_2-Sb anodes. Chemosphere 205 (2018) 361.

[32] V. K. Sharma, R. Zboril, R. S. Varma, Ferrates: greener oxidants with multimodal action in water treatment technologies, Accounts. Chem. Res. 48 (2015) 182.

[33] M. Panizza, A. Kapalka, C. Comninellis. Oxidation of organic pollutants on BDD anodes using modulated current electrolysis, Electrochim. Acta. 53 (2008) 2289.

[34] Y. M. Liu, S. Chen, X. Quan, H. T. Yu, H. M. Zhao, Y. B. Zhang, Efficient Mineralization of Perfluorooctanoate by Electro-Fenton with H_2O_2 Electro-generated on Hierarchically Porous Carbon, Environ. Sci. Technol. 49 (2015) 13528.

[35] M. Alsheyab, J. Qian. Jiang, C. Stanford, Electrochemical generation of ferrate (VI): Determination of optimum conditions, Desalination. 254 (2010) 175.

[36] S. Licht, X. Yu, Electrochemical alkaline Fe(VI) water purification and remediation, Environ. Sci. Technol. 39 (2005) 8071.

[37] X. Xie, Y. Hu, H. Cheng, Rapid degradation of p-arsanilic acid with simultaneous arsenic removal from aqueous solution using Fenton process, Water Res. 89 (2016) 59.

[38] J. E. Toth, K. A. Rickman, A.R. Venter, J. J. Kiddle, S. P. Mezyk, Reaction kinetics and efficiencies for the hydroxyl and sulfate radical based oxidation of artificial sweeteners in water, J. Phys. Chem. A. 116 (2012) 9819.

[39] W. Ren, Q. L. Peng, Z. A. Huang, Z. H. Zhang, W. Zhan, K. L. Lv, J. Sun. Effect

of Pore Structure on the Electro-Fenton Activity of ACF@OMC Cathode, Ind. Eng. Chem. Res. 54 (2015) 8492.

[40] S. Khan, X. X. He, J. Ali. Khan, H. M. Khan, D. L. Boccelli, D. D. Dionysiou, Kinetics and mechanism of sulfate radical and hydroxyl radical-induced degradation of highly chlorinated pesticide lindane in UV/peroxymonosulfate system, Chem. Eng. J. 318 (2017) 135.

[41] X.P. Zhu, S. Y. Shi, J. J. Wei, F. X. Lv, H. Z. Zhao, J. T. Kong, Q. He, J. R. Ni, Electrochemical oxidation characteristics of p-substituted phenols using a boron-doped diamond electrode, Environ. Sci. Technol. 41 (2007) 6541.

[42] D. Lakshmanan, D. A. Clifford, G. Samanta, Ferrous and Ferric Ion Generation During Iron Electrocoagulation, Environ. Sci. Technol. 43 (2009) 3853.

[43] Y. J. Long, H. Li, X. Xing, J. R. Ni, Enhanced removal of Microcystis aeruginosa in BDD-CF electrochemical system by simple addition of Fe^{2+}, Chem. Eng. J. 325 (2017) 360.

[44] X. H. Sun, Q. Zhang, H. Liang, L. Ying, X. X. Meng, V. K. Sharma, Ferrate(VI) as a greener oxidant: Electrochemical generation and treatment of phenol, J. Hazard. Mater. 319 (2016) 130.

[45] Z. S. Wu, S. B. Yang, Y. Sun, K. Parvez, X. L. Feng, K. Mullen, 3D Nitrogen-Doped Graphene Aerogel-Supported Fe_3O_4 Nanoparticles as Efficient Electrocatalysts for the Oxygen Reduction Reaction, J. Am. Chem. Soc. 134 (2012) 9082.

Figure Captions:

Figure 1 Evolution of *p*-NP residual percentage (a), COD residual percentage (b) under original pH condition (pH=5.6); evolution of *p*-NP residual percentage (c), COD residual percentage (d) under an acidic pH condition (pH=3); and evolution of the *p*-NP residual percentage (e), COD residual percentage (f) under an alkaline pH condition (pH=11) in the BDD-Fe_c-CF system compared with a traditional electrochemical systems (BDD-SS) and (BDD-CF). Initial *p*-NP concentration: 1 mmol; electrolyte: 0.2 M Na_2SO_4; 250 ml; constant current density was 20 mA cm^{-2}.

Figure 2 Oxidation contributions identification for BDD-Fe_c-CF system by COD degradation efficiency under original, acidic and alkaline conditions. AO: anodic oxidation; EO: oxidation of electro-generation groups, EF: Electro-Fenton, Fe(VI): oxidation by ferrate (Fe(VI)). Flocs: removed by coagulation.

Figure 3 Concentration of ·OH (a) and other electro-generated oxidants (b) under different pH conditions of original (pH=5.6), acidic (pH=3), and alkaline (pH=11) in BDD-Fe_c-CF system. The error bars represent the standard deviation of the three group of repeated experiments. Electrolyte: 0.2 M Na_2SO_4; 250 mL; constant current density: 20 mA cm^{-2}.

Figure 4 Behavior of Fe ions in BDD-Fe_c-CF system.

Figure 5 Evolution of Fe^{2+} concentration (a) and Fe^{3+} concentration (b) in aqueous solution; Fe^{2+} and Fe^{3+} absorbed on carbon felt cathode (c) and pH values under different current densities with electrolysis time (d) in the BDD-Fe_c-CF system under acidic conditions. Electrolyte: 0.2 M Na_2SO_4; 250 mL.

Figure 6 Concentration of total Fe ions in BDD-Fe_c-CF system under alkaline conditions after 1 h of electrolysis under different current densities. Electrolyte: 0.2 M Na_2SO_4; 250 mL.

Figure 1

Click here to download high resolution image

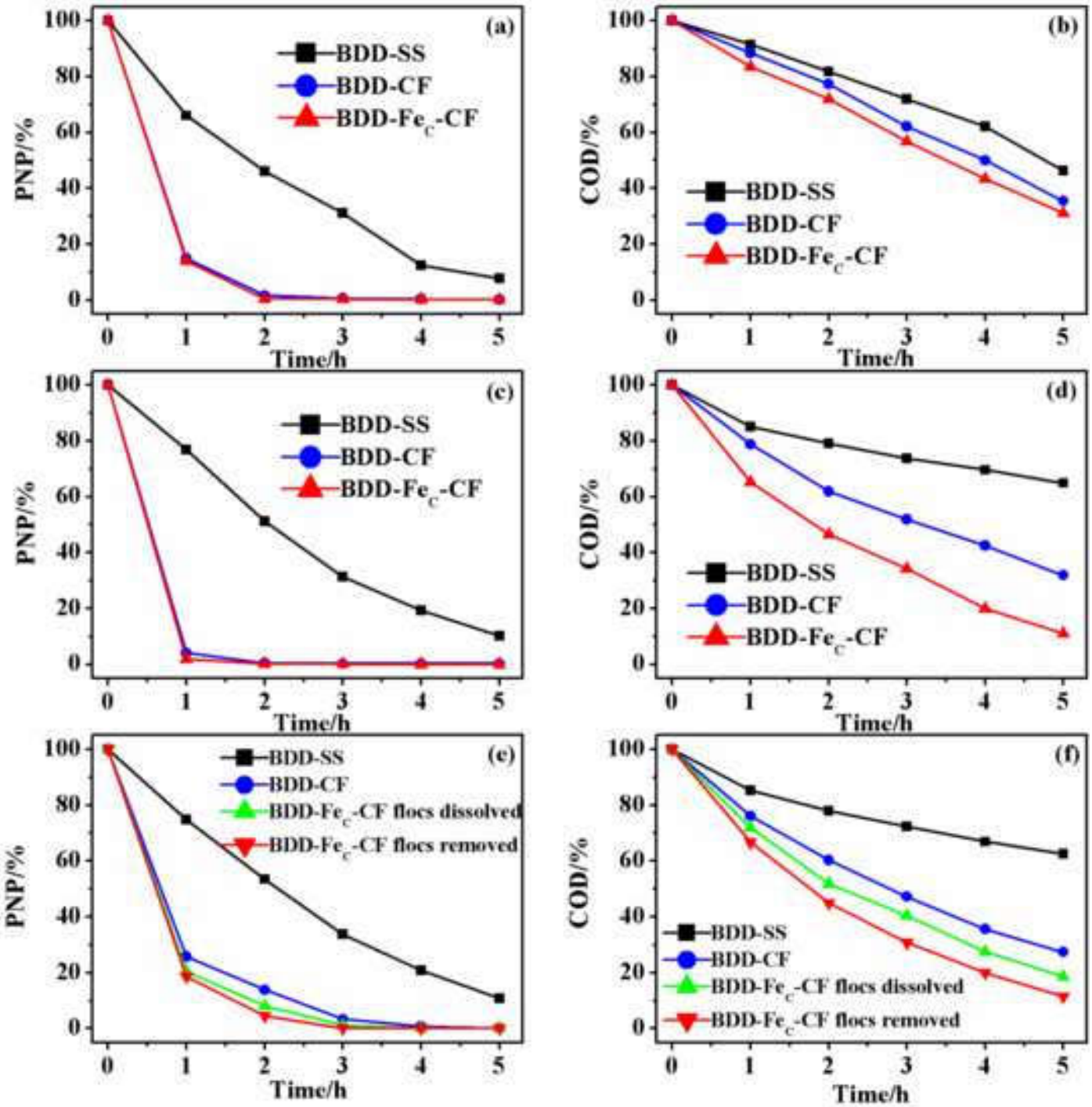

Figure 2
Click here to download high resolution image

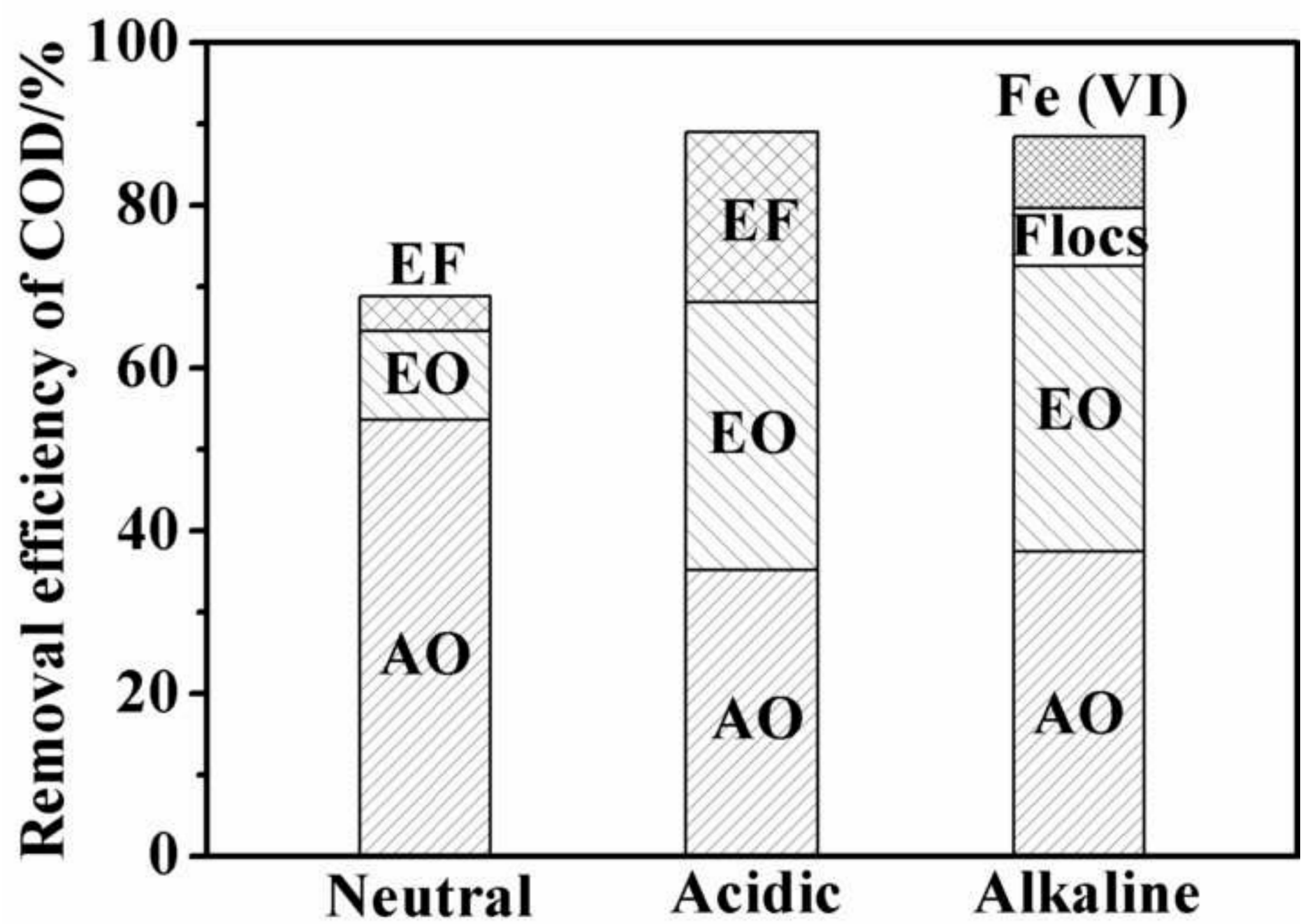

Figure 3
Click here to download high resolution image

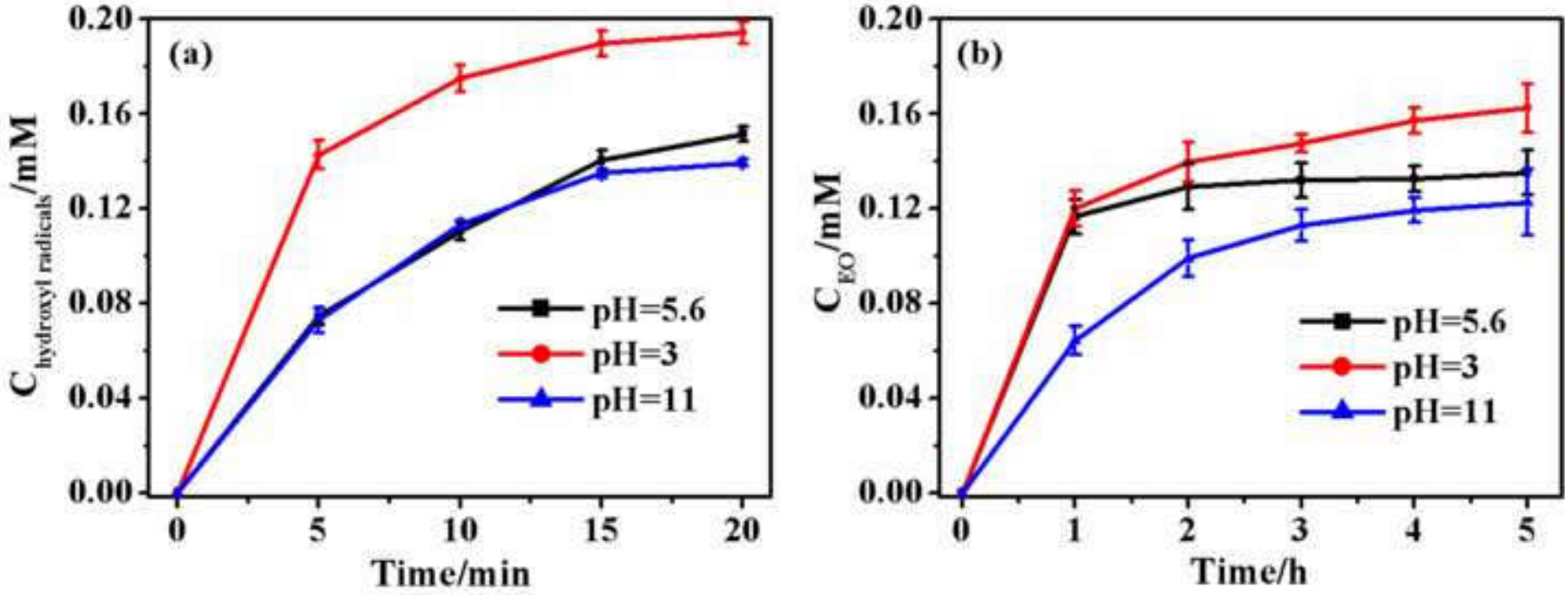

Figure 4
Click here to download high resolution image

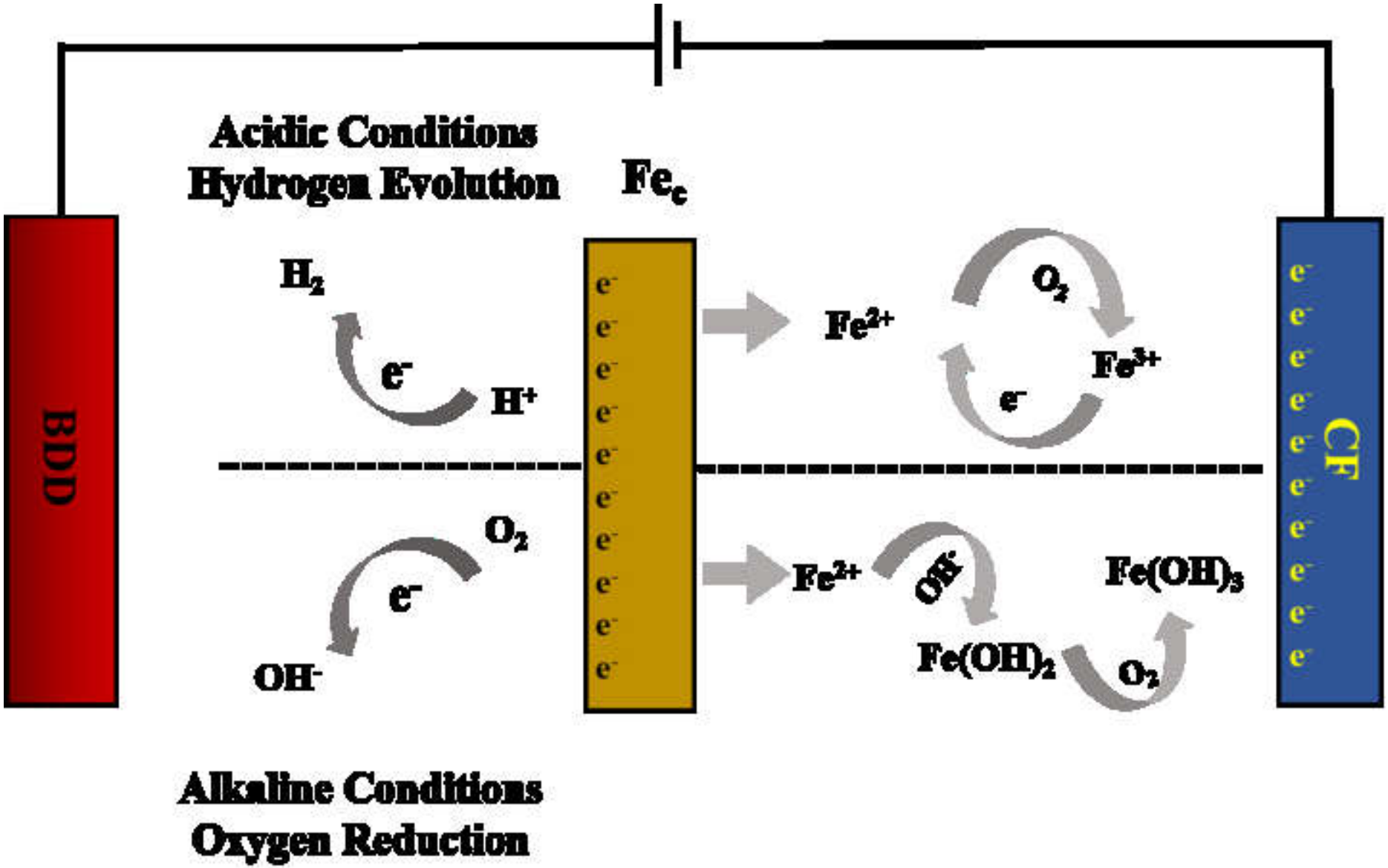

Figure 5

Click here to download high resolution image

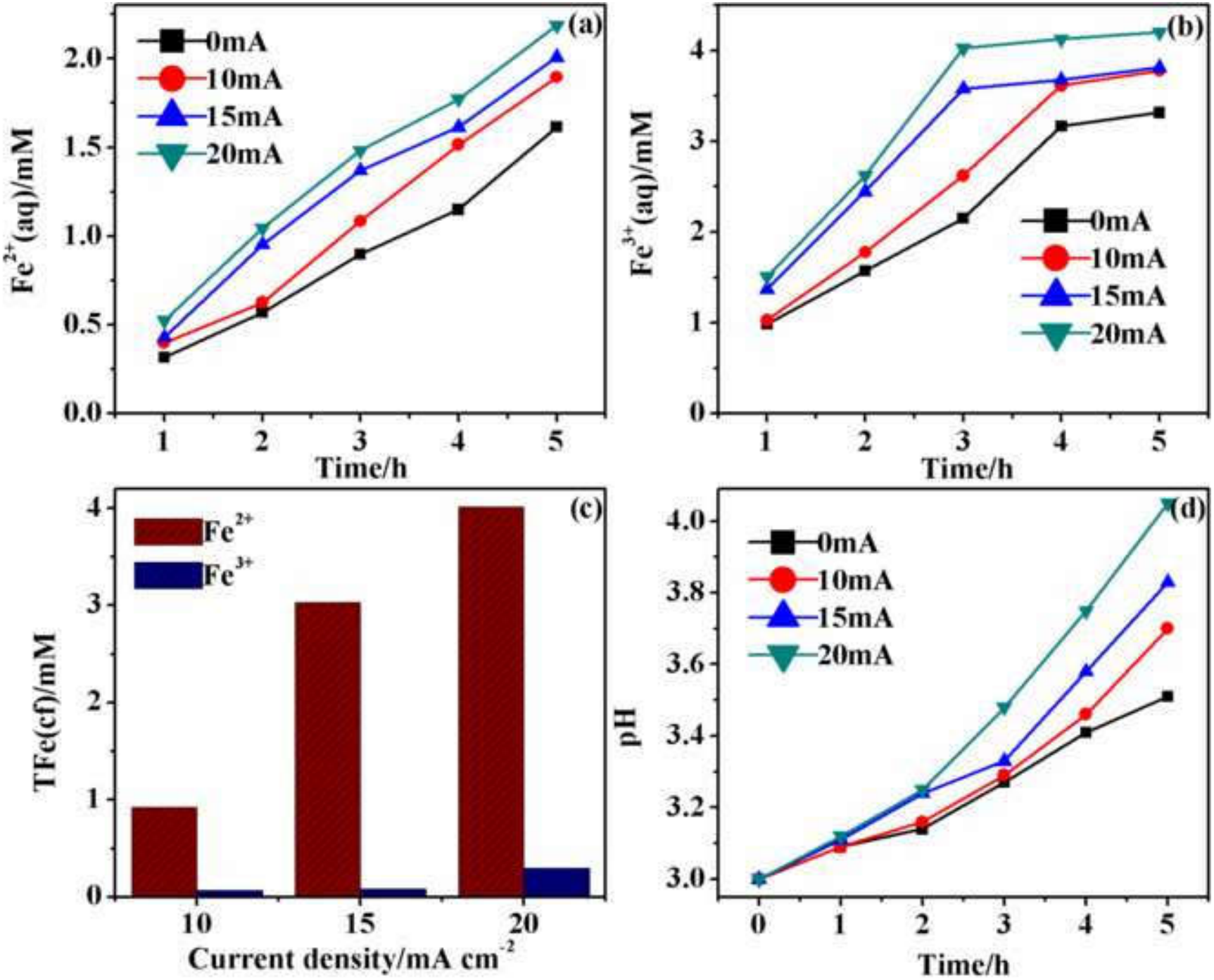

Figure 6
Click here to download high resolution image

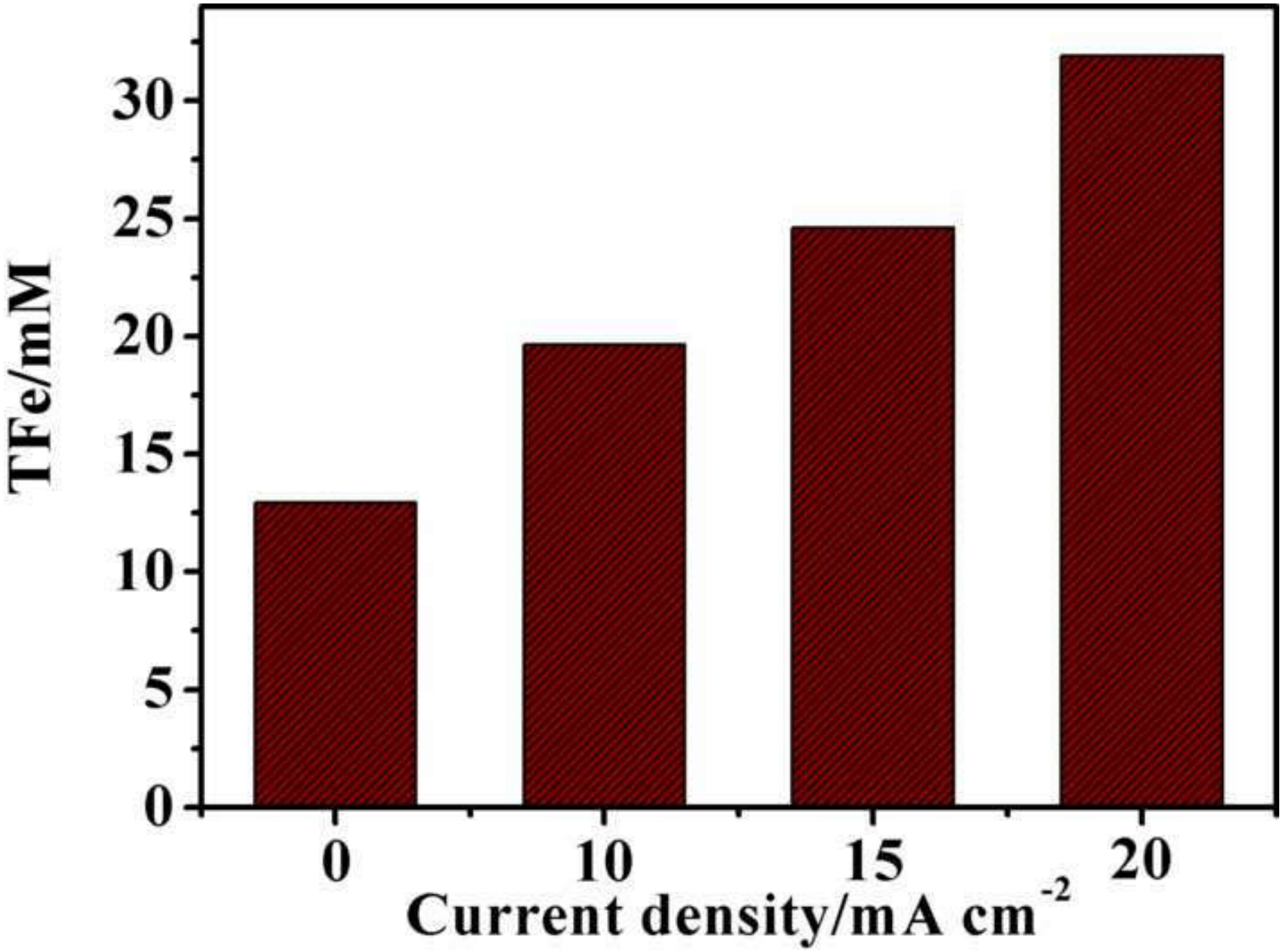

Supplementary Materials

Click here to download Supplementary Materials: Supporting Information.doc